2024 European Control Conference (ECC)
June 25-28, 2024. Stockholm, Sweden

Super-twisting algorithm with anti-windup applied to a wave energy converter

F. D. Mosquera, N. Faedo, C. A. Evangelista and P. Puleston

Abstract— **The development of effective control strategies is essential to advance the commercialisation of wave energy converters by maximising energy capture. This study employs a novel control approach integrating an optimal control term, based on so-called moments, with a tracking term rooted in second-order sliding mode control. The optimal term determines the control action to optimise energy conversion under nominal conditions and provides an optimal velocity reference. Subsequently, a Super-twisting algorithm is deployed to robustly track the optimal reference. However, challenges of integral windup may arise when employing the Super-twisting algorithm within the tracking loop under conditions of actuator saturation. To address this, the paper implements two anti-windup techniques aimed at mitigating the windup effect in the Super-twisting algorithm. Simulation results validate the effectiveness of the proposed modification to the main control strategy in dealing with saturated actuators.**

I. Introduction

The global development of wave energy converters (WECs) remains in its early stages. Based on assessments using wind and wave models, experts estimate the global theoretical potential of wave energy to be around 3 TW of available power [1], equivalent to an annual generation of 29,500 TWh according to the International Renewable Energy Agency [2]. For context, the total global primary energy production in 2022, across all energy sources, was 28,527 TWh [3].

The advancement of wave energy technology has been slow primarily due to challenges such as survivability in severe sea conditions and uncertainty in device concepts. In addition, the substantial costs and rigorous testing requirements pose obstacles to large-scale deployment. In response to these challenges, control technology emerges as a critical factor in optimising wave energy converter performance by adapting to diverse wave conditions and collaborating with power take-off mechanisms [4].

This study focuses on an automatic control strategy which maximises energy extraction in WECs while considering their physical constraints. This control strategy combines an optimal control technique based on moments, which calculates the control action and the optimal motion of the device based on the force exerted by the wave, with a control loop that ensures the robust operation of the equipment according to the calculated optimal reference motion. In this sense, sliding modes have been used for the robust control loop, and for this reason, the strategy has been named Sliding Mode Moment-based Control (SM^{2}C).

The SM^{2}C strategy, which incorporates the Super-twisting algorithm for the tracking loop, belonging to the family of second-order sliding modes, has been presented and validated in simulation environments [5], as well as in a hardware-in-the-loop system [6]. The purpose of this study is to extend this control strategy to test it in a wave tank using prototypes similar to the Wavestar [7], which has been used to generate the SWELL database [8], [9].

The Super-twisting algorithm (STA) stands out as a well-established second-order sliding mode control approach, particularly effective for systems affected by certain types of disturbances that are Lipschitz continuous with respect to time [10], [11]. Notably, STA is specifically applied to systems with relative degree one concerning the control input and has the advantage of dispensing the measurement of the sliding function derivative, a requirement for other second-order sliding mode algorithms [12].

However, when the control input is executed through a saturating actuator, the signal produced by the conventional Super-twisting controller may exceed the saturation limits, leading to the windup effect due to the integral action of the controller. To counteract or prevent this effect in the Super-twisting algorithm, various solutions have been proposed in the existing literature [11], [13]–[15].

Among these solutions, this study incorporates two of main strategies: Golkani et al., [11], propose the addition of a damping term in the integral term of the STA, while Seeber et al., [16], present a conditioned algorithm that modifies the traditional STA structure without altering its response when operating below the saturation limits. Consequently, the focus of this study is to demonstrate the integration of this adapted approach into the SM^{2}C control structure, incorporating into the Super-twisting tracking term the possibility of working with saturating actuators.

A. Notation

Throughout this paper, vectors are indicated with lower-case bold characters, $\boldsymbol{x}$, while scalar elements are indicated with lower-case italic characters, such as k, l, m. Matrices are

F. D. Mosquera, C. A. Evangelista and P. F. Puleston are with the Instituto LEICI, Fac. de Ingeniería/UNLP - CONICET, La Plata, Bs.As., Argentina. F. D. Mosquera is also with the Center of Offshore Energy Research (COER), Maynooth University, Ireland. (email: facundo.mosquera@mu.ie).

N. Faedo is with the Marine Offshore Renewable Energy (MORE) lab, Department of Mechanical and Aerospace Engineering, Politecnico di Torino, Torino, Italy.

F. D. Mosquera, C. A. Evangelista and P. F. Puleston are funded by Facultad de Ingeniería, CONICET and ANCyT. F. D. Mosquera is also funded by MaREI, the SFI Research Centre for Energy, Climate and Marine,, under Grant No. 12/RC/2302 P2.

N. Faedo has received funding from the European Union's Horizon 2020 research and innovation programme under the MarieSklodowska-Curie grant agreement No 101024372.

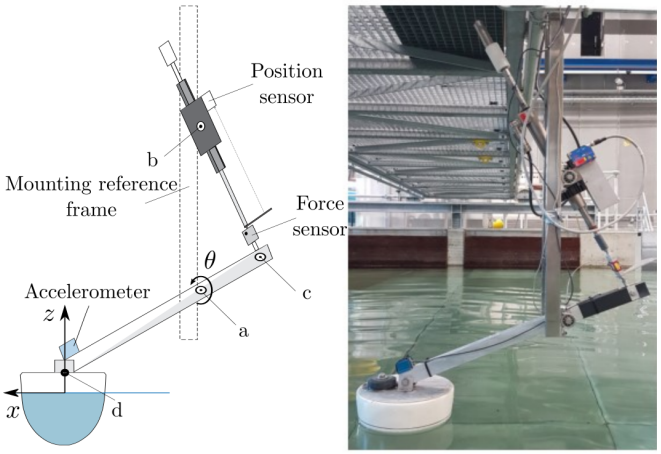

Figure 1. 1:20 scale prototype of the Wavestar device (left) and its schematic (right).

denoted with bold capital letters, e.g., $\mathbf{A}$, and $\mathbb{R}^{n\times m}$ denotes real matrices with n rows and m columns. Additionally, the variable $u^* = \text{sat}_\rho(u)$, where $\text{sat}_\rho(u)$ is the saturated value of the variable u in $\pm\rho$. Finally, the abbreviation $\lfloor\sigma\rceil^p = |\sigma|^p\text{sign}(\sigma)$ is used, with $\lfloor\sigma\rceil^0 = \text{sign}(\sigma)$.

B. Paper organisation

The remainder of this study is presented as follows: in Section II, the model of the prototype under study is described through identification. In Section III, the SM^{2}C control structure with the addition of the anti-windup (AW) term is presented. The results with this control structure are shown in Section IV, and the conclusions of the study are presented in Section V.

II. Model

The system to be controlled in this work is a 1:20 scale prototype of a Wavestar-type wave energy converter (WEC) (see Figure 1). To obtain the system model, a black-box identification is carried out, following the approach proposed by [17], to capture the relevant dynamics for control design. This identification allows the representation of the system's key characteristics and provides the necessary basis for the design of effective control strategies.

It is worth mentioning that a model could have been obtained by numerical characterisation based on boundary element methods (BEM) using linear potential theory [18]. However, as mentioned in [17], this approach only focuses on hydrodynamics, ignoring any nonlinear physical characteristics associated with the experimental nature of the system, such as friction effects in the power take-off (PTO) system that generate dead zones for device motion (see [8]).

Here, the experiment performed in [8] is described to facilitate the understanding of the control-oriented model identified, which then has been used for control design purposes. In particular, for the identification experiment, a set of down-chirp-type input signals (torque) $f_{\text{ID}}(t)$ is designed, whose amplitudes vary between experiments but are always generated in a frequency range $\mathcal{W}_{ID} = [\omega_i, \omega_f] \subset \mathbb{R}^+$. The use of a descending chirp instead of the more commonly used ascending chirp is because it is considered that this way the effect of radiated waves on the experimental results is minimized, as mentioned in [17], [19].

Once the known input to the system is defined, the identification experiment is carried out as follows: In calm water, that is, without the presence of waves in the tank, the designed input is applied through the PTO system, measuring the velocity produced by the device, ν_{ID}, as the output of interest. With this information, a non-parametric characterisation in the frequency domain is generated by calculating the estimation of the average empirical transfer function (EFTE) [20] as follows:

$$\begin{aligned}\bar{G}_\theta(j\omega) &= \frac{1}{N}\sum_{p\in\mathcal{N}_N}\tilde{G}^p_\theta(j\omega),\\ \tilde{G}^p_\theta(j\omega) &= \frac{V^p_{ID}(j\omega)}{F^N_{ID}(j\omega)},\end{aligned} \tag{1}$$

where $\bar{G}_\theta(j\omega) \in \mathbb{C}^N$ and $\tilde{G}^p_\theta(j\omega) \in \mathbb{C}^N$, with the superscript ^{p} indicating that this EFTE is associated with the amplitude of the chirp A_p.

Once $\bar{G}_\theta(j\omega)$ is calculated, standard system identification techniques can be used to approximate the corresponding response operator. In this case, subspace-based techniques are used (see [21]), which provide a finite-dimensional strictly proper continuous-time state-space model:

$$\Sigma_{ID-\theta} \equiv \begin{cases}\dot{\boldsymbol{x}} &= \mathbf{A}\boldsymbol{x} + \mathbf{B}(f_\theta - u)\\ \nu_\theta &= \mathbf{C}\boldsymbol{x}\end{cases} \tag{2}$$

with $G_{ID-\theta}(s) := \mathbf{C}(s\mathbf{I}-\mathbf{A})^{-1}\mathbf{B}$, $\boldsymbol{x}$ represents the states of a black-box identification, f_θ is the excitation torque, u is the control torque, ν_θ is the angular velocity and system output, the triplet $(\mathbf{A},\mathbf{B},\mathbf{C}) \in \mathbb{R}^{n\times n}\times\mathbb{R}^{n\times 1}\times\mathbb{R}^{1\times n}$ is minimal, and the system (2) is asymptotically stable.

Figure 2 shows the Bode diagram corresponding to the average empirical transfer function of the identified device,

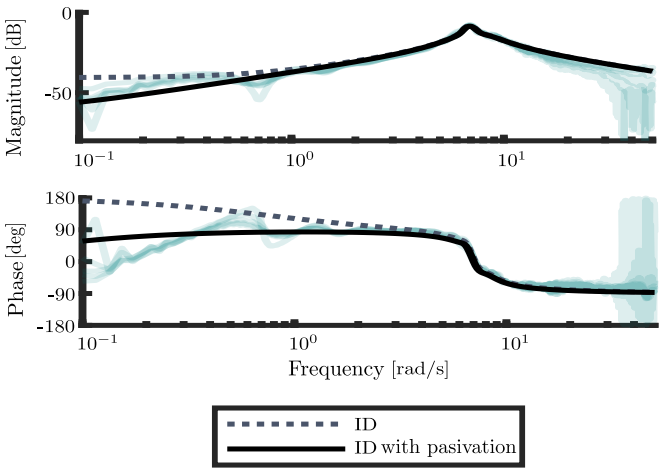

Figure 2. Bode diagram of the frequency response for the average empirical transfer function.

calculated for each experiment performed (green lines with transparency), along with the characteristic response of the identified model $G_{ID-\theta}$ (gray dashed line). Additionally, the frequency response of the passivated model is presented in the same figure (solid black line). The system passivation is carried out following the methodology proposed in [21], to fulfil the condition of real positivity. This condition is essential to guarantee the existence and uniqueness of energy maximization solutions using moment theory in optimal control calculation.

III. Control structure

In this section, the SM^{2}C control scheme with AW is presented, and the control blocks which compose the structure are described in this section, namely, the moment-based optimal control and both Super-twisting algorithms with anti-windup.

The SM^{2}C control strategy is composed of two terms:

$$u(t) = u_{\text{opt}}(t) + u_{\text{STA}}(t) \tag{3}$$

where the first term, u_{opt}, is an optimal control term, calculated to maximise energy extraction from the WEC under nominal operating conditions. The second term, u_{STA}, is a term that allows robust reference tracking, ensuring that the system will maintain the conditions for which the maximization is calculated despite system uncertainty and possible disturbances.

A. Design of the optimal control term

In wave energy extraction, the design of optimal control involves a maximization criterion that aims to absorb as much energy as possible from ocean waves within finite time intervals $\mathcal{T} = [kT, (k+1)T] \subset \mathbb{R}^+$, where $k \in \mathbb{N}$ and T is the period along which the energy maximisation is considered. The energy absorbed from the waves is converted into PTO system energy and can be directly calculated as the time integral of the instantaneous converted power. Therefore, this control procedure can be formulated as an optimal control problem with the objective function $\mathcal{J} : \mathbb{R} \to \mathbb{R}$ defined as:

$$\mathcal{J}(u_{\text{opt}}) = \frac{1}{T}\int_{\mathcal{T}} u_{\text{opt}}(\tau)\nu_\theta(\tau)d\tau, \tag{4}$$

where $u_{\text{opt}} : \mathcal{T} \to \mathbb{R}$ is the control force of the PTO. The set of constraints can be formulated as:

$$\mathscr{C} : \begin{cases} \nu_\theta(t) & \leqslant V_{\max}, \\ u_{\text{opt}}(t) & \leqslant U_{\max}, \end{cases} \tag{5}$$

where $t \in \mathcal{T}$, and $\{V_{\max}, U_{\max}\} \subset \mathbb{R}^+$.

With the objective function defined in (4) and the set of state constraints defined in (5), the optimal control problem (OCP) can be formulated as:

$$\begin{aligned} u_{\text{opt}} &= \arg\max_{u\in\mathscr{U}} \mathcal{J}(u) \\ &\text{subject to:} \\ &\begin{cases} \text{WEC dynamics } \Sigma_{ID-\theta} \\ \text{state and input constraints } \mathscr{C} \end{cases} \end{aligned} \tag{6}$$

where $\mathscr{U}$ denotes the set of admissible inputs and the system $\Sigma_{ID-\theta}$ describes the motion dynamics of the device, i.e., equation (2).

The moment-based technique is used to express the system's steady-state response in terms of moments, which are specific solutions of an invariant equation. This technique allows for translating the energy maximization problem, which has infinite dimensions, into a finite-dimensional optimization program. In the framework of the moment-based optimal control described in this section, the energy maximization problem is transformed into a strictly convex quadratic program (QP) [22], which systematically guarantees a unique solution for maximizing energy. Furthermore, this solution simultaneously satisfies the constraints imposed on the control input and the states [23]. This approach has a significant impact on the practical feasibility of moment-based control as it facilitates the use of QP solvers, resulting in a computationally efficient control solution.

The reference generation procedure can be summarized in the following steps [24]:

1) Determine the set of solutions $\mathcal{R} : \{u_{\text{opt}}, \nu_{\theta_{\text{opt}}}\}$ by solving the OCP (6) within a time period $\Xi_K = [K\Delta_{\text{h}}, K\Delta_{\text{h}} + T_h] \subset \mathbb{R}$, $K \in \mathbb{N}$, where T_{h} is the horizon for which (4) is effectively maximised, and Δ_{h} is the mobile horizon step.
2) Provide the set $\mathcal{R}$ to the tracking control loop within the interval $[K\Delta_{\text{h}},\ (K+1)\Delta_{\text{h}}] \subset \mathbb{R}^+$, within a mobile horizon interval Δ_{h}.
3) Advance $\Xi_K \mapsto \Xi_{K+1}$ and return to 1).

B. Design of the tracking term

The tracking control term is designed to ensure that the system behaves according to the reference provided by the moment-based optimal control. For this purpose, a sliding variable of the form is proposed:

$$\sigma(\boldsymbol{x}, t) = \nu_{\theta_{\text{opt}}}(t) - \nu_\theta(t) = \nu_{\theta_{\text{opt}}}(t) - \mathbf{C}\boldsymbol{x}(t), \tag{7}$$

This sliding variable has a relative degree of 1 for the control input u in the system model (2), meaning that its first derivative can be written as:

$$\begin{aligned} \dot\sigma(\boldsymbol{x}, t) &= \dot\nu_{\theta_{\text{opt}}}(t) - \mathbf{CA}\boldsymbol{x}(t) - \mathbf{CB}u(t) = \\ &= \dot\nu_{\theta_{\text{opt}}}(t) - \mathbf{CA}\boldsymbol{x}(t) - \mathbf{CB}u_{\text{opt}}(t) - \mathbf{CB}u_{\text{STA}}(t) = \\ &= a(\boldsymbol{x}, t) + b(t)u_{\text{STA}}(t). \end{aligned} \tag{8}$$

Among second-order sliding mode algorithms, the Super-Twisting algorithm (STA) is the most commonly used for working with sliding variables of relative degree 1 with respect to the control input. The STA, as proposed in [10], has the following structure:

$$u_{\text{STA}}(t) = k_1\lfloor\sigma(t)\rceil^{1/2} + v(t) \tag{9a}$$

$$\dot v(t) = k_2\lfloor\sigma(t)\rceil^0 \tag{9b}$$

where k_1 and k_2 are the constant gains of the algorithm.

The Super-twisting algorithm uses an integral to generate a continuous control signal, as shown in equation (9). However, when this signal is applied to a saturating actuator and

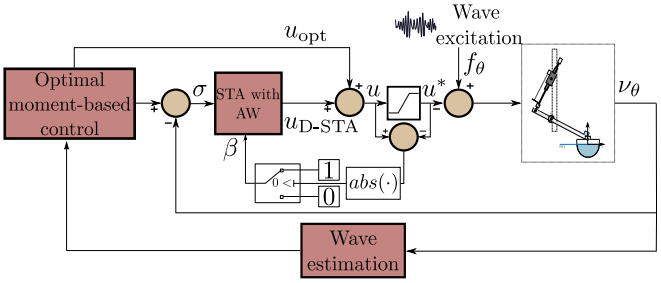

Figure 3. SM^{2}C control scheme with the damped anti-windup proposal, the damped anti-windup is from [11].

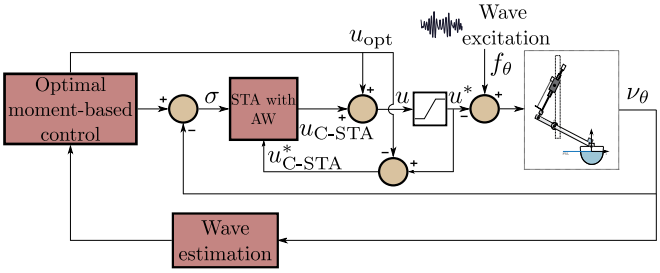

Figure 4. SM^{2}C control scheme with the conditioned anti-windup proposal, this technique is an adaptation of [16].

the control action calculated by the algorithm exceeds the actuator limits, the system enters open-loop and the integral term continues to accumulate the generated error, leading to the phenomenon of integral windup.

To address this issue, this study implements two diverse proposals to compare and contrast their advantages and disadvantages.

1) Damped anti-windup proposal: The study published in [11] modifies the structure of the conventional Super-twisting algorithm to account for the effect of integral windup in the control design adding a damping term in the algorithm integral[1]:

$$u_{\text{D-STA}} = k_{\text{D}_1}\lfloor\sigma\rceil^{1/2} + v_{\text{D}}, \tag{10a}$$

$$\dot{v}_{\text{D}} = k_{\text{D}_2}\lfloor\sigma\rceil^{0} + k_{\text{D}_3}\beta v_{\text{D}}, \tag{10b}$$

which ends up in a damped STA (D-STA). This modification requires that the state v satisfies an initial condition $|v_0| \leqslant \frac{k_2}{k_3}$, which, as it represents the integral state of the control algorithm, is simple to verify. β is a binary variable that is determined based on the saturation value:

$$\beta = \begin{cases} 1 & \text{if } |u| > \rho, \\ 0 & \text{if } |u| \leqslant \rho, \end{cases} \tag{11}$$

where ρ is the saturation value of the actuator. A representative scheme of the algorithm working principle can be observed in Figure 3.

Through a stability analysis [11], it is proven that the gains of the algorithm in (10) must satisfy:

$$k_1 > 2\sqrt{\frac{k_2\rho}{b_m\rho - a_M}} \quad k_2 > \frac{L_a + L_b a_M}{b_m^2} \quad \frac{k_2}{k_3} \leqslant \rho \tag{12}$$

where a_M, L_a, b_m, and L_b are known constants that bound the amplitude and variation of the functions a and b, ensuring that these functions are globally bounded and Lipschitz continuous, i.e.:

$$\begin{aligned} |a(\boldsymbol{x},t)| \leqslant a_M \quad \left|\frac{da(\boldsymbol{x},t)}{dt}\right| \leqslant L_a \quad \forall t > 0 \\ 0 < b_m \leqslant b(t) \leqslant 1 \quad \left|\frac{db(t)}{dt}\right| \leqslant L_b \quad \forall t > 0 \end{aligned} \tag{13}$$

[1]Henceforth, the dependency on t is omitted wherever possible to conserve space.

Calculating the gains of the algorithm based on the mentioned bounds ensures that the system converges to the origin in finite time, even in the presence of uncertainty and disturbances. Additionally, it generates a continuous control action throughout the domain, guaranteeing that if its absolute value exceeds saturation, the windup effect is mitigated.

It should be noted that the specified constraint for the term $b(t)$, specifically $b(t) < 1$, may not be satisfied in all systems.

2) Conditioned anti-windup proposal: The anti-windup strategy, introduced in [16], is developed using the conditioning technique proposed in [25]. This technique involves computing a modified reference signal, denoted as r^*, such that applying r^* to the controller instead of the original reference signal r results in $u = u^*$. This approach effectively mitigates windup by ensuring that the controller with the modified reference r^* behaves as if actuator saturation is not present [16].

Considering equation (9a) and assuming $\nu_{\theta_{\text{opt}}} = r$, a realizable reference signal r^* satisfies:

$$u^*_{\text{C-STA}} = k_{\text{C}_1}\lfloor r^* - \nu_\theta\rceil^{1/2} + v_{\text{C}}. \tag{14}$$

The conditioned control law is then derived by substituting r with r^* in the dynamic part of the algorithm (9), yielding:

$$\dot{v}_{\text{C}} = k_{\text{C}_2}\lfloor r^* - \nu_\theta\rceil^{0}. \tag{15}$$

By subtracting v_{C} and taking the sign of both sides of (14), we observe that $\lfloor r^* - \nu_\theta\rceil^0 = \lfloor u^*_{\text{C-STA}} - v_{\text{C}}\rceil^0$ holds. Thus, the conditioned STA is derived as:

$$u_{\text{C-STA}} = k_{\text{C}_1}\lfloor\sigma\rceil^{1/2} + v_{\text{C}}, \tag{16a}$$

$$\dot{v}_{\text{C}} = k_{\text{C}_2}\lfloor u^*_{\text{C-STA}} - v_{\text{C}}\rceil^{0}, \tag{16b}$$

$$u^*_{\text{C-STA}} = u^* - u_{\text{opt}}, \tag{16c}$$

where u is the total control action from (3) and $\sigma = \nu_{\theta_{\text{opt}}} - \nu_\theta$ from (7). The previous deduction and convergence of the conditioned STA (C-STA) for a simplified model are provided in [16]. The stability of the conditioned STA with given non-negative bounds W and L, and a control input bound ρ is obtained when the following inequalities are fulfilled [16]:

$$k_{\text{C}_1} > \sqrt{2k_{\text{C}_2}\frac{(\rho + W)}{(\rho - W)}} \quad k_{\text{C}_2} > L \tag{17}$$

Finally, a schematic illustrating the working principle of the C-STA is depicted in Figure 4.

IV. Simulation Results

This section presents the simulation results of the SM^{2}C control strategy with anti-windup. The tests shown are performed using the identified model of the physical system as described in Section II, and the input used to excite the system is the excitation torque obtained from the SWELL database [8], [9], which provides experimental measurements. The control gains were calculated considering uncertainties (in the parameters) of up to 15% in the identified system. These gain values for the different algorithms along with the parameters for the model identification, the model order and the actuator saturation value are depicted in Table I.

TABLE I
System and control parameters

Control algorithms	System & actuator
k_1 = 7	n = 6
k_2 = 10	ω_i = 0.1 rad/s
k_{D_1} = 7	ω_f = 30 rad/s
k_{D_2} = 10	N = 5
k_{D_3} = 0.95	ρ = 11Nm
k_{C_1} = 7	
k_{C_2} = 10	

The torque responsible for moving the device is applied to the system using the values recorded in the experimental campaign [8]. For the simulation, a period of 200 s is considered with a step equal to the sampling period used in the experiment, i.e., $T_s = 1/200$ s. The optimal moment-based control system utilises the excitation torque data to generate a real-time velocity reference to maximise energy extraction for the given input. Subsequently, the tracking control mechanism ensures effective tracking of this optimal reference. To assess the algorithm convergence to the surface ($\sigma = \dot{\sigma} = 0$), the control action is activated in the simulation at $t = 10$ s. Figure 5 illustrates a comparison of the sliding variables of the three Super-twisting algorithms STA, D-STA, and C-STA.

Furthermore, Figure 6 illustrates the convergence of the algorithms to the surface in the phase plane, where it can be observed that the three algorithms have the same convergence pattern because in this phase the control action is below the saturation value.

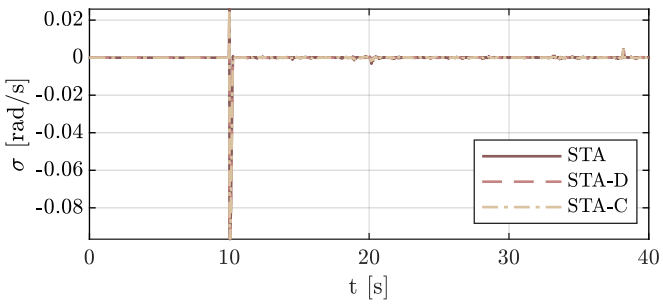

Figure 5. Sliding variable evolution in the first 40 s for the different algorithms. STA is the Super-twisting algorithm without an anti-windup technique, D-STA is the algorithm with a damped anti-windup technique and C-STA is the algorithm with a conditioned Super-twisting technique.

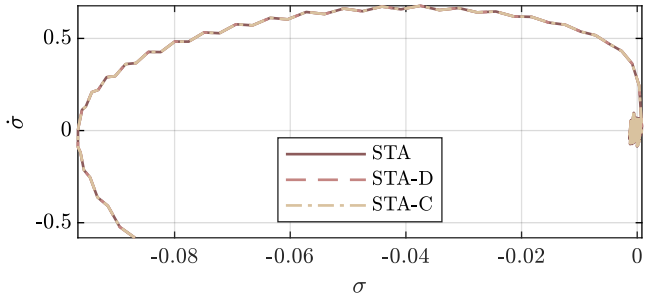

Figure 6. Convergence of the Super-twisting algorithms to the origin of the phase plane $\sigma - \dot{\sigma}$.

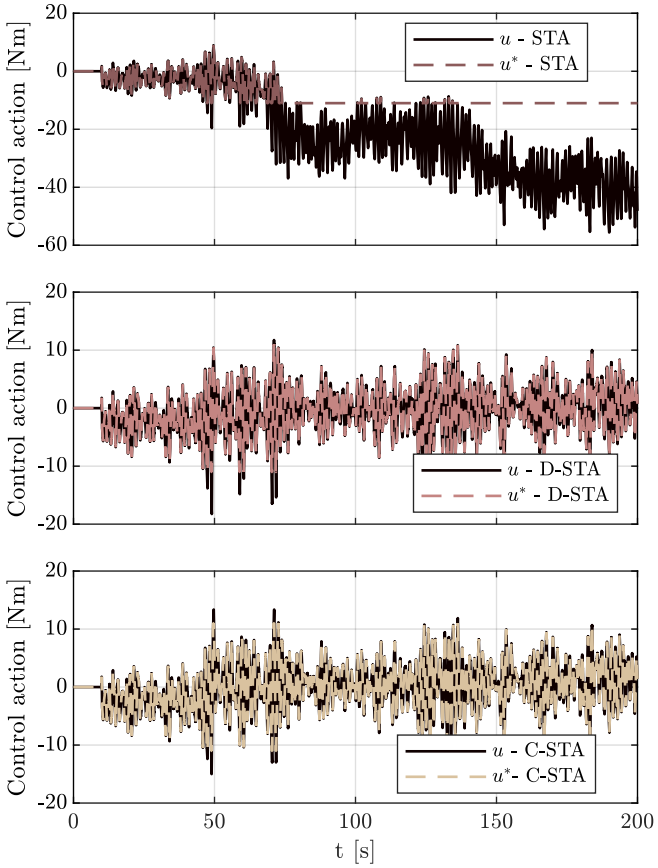

Figure 7. Calculated (u) and applied (u^*) control actions for each algorithm. First row: STA without anti-windup. Second row: D-STA. Third row: C-STA.

Finally, Figure 7 illustrates the calculated (u) and applied (u^*) control actions for each algorithm compared in this study. Specifically, it is observed that for this application, particular uncertainty and actuation time (equivalent to T_s), the Super-twisting algorithm without anti-windup fails to maintain the system on the surface due to its unproven persistence when saturated. Thus, the traditional STA is ineffective for the application under study in this work. Additionally, both algorithms which incorporate anti-windup techniques, the D-STA and the C-STA, effectively maintain the system on the surface.

V. Conclusions

In this study, two techniques are employed to address integral windup in the Super-twisting algorithm, crucial for controlling a wave energy converter with saturated actuators. The Super-twisting algorithm is integrated into a broader control framework comprising an optimal moment-based control element with a robust sliding mode tracking component. Specifically, under conditions of actuator saturation, challenges of integral windup can be encountered when utilising the Super-twisting algorithm within the tracking loop due to the integral term in the algorithm.

The primary objective of the main control strategy in this work, i.e., sliding mode moment-based control, is to enhance energy extraction efficiency from a wave energy conversion device. Through simulation experiments, both windup mitigation techniques demonstrate effectiveness. Despite instances of control actions surpassing actuator limits, the control action is swiftly readjusted, ensuring the uninterrupted pursuit of the reference trajectory for maximising energy extraction.

Among the anti-windup techniques considered, even with both algorithms demonstrating good performance, it is observed that the algorithm which incorporates damping into the integral term requires an additional gain to ensure convergence during saturation recovery. Moreover, the damped Super-twisting algorithm necessitates restrictive bounds to demonstrate convergence. In contrast, the conditioned technique successfully attains anti-windup objectives with equivalent gains to the traditional Super-twisting algorithm, requiring only structural modifications and adjustments in how the bounds are computed.

References

[1] G. Mork, S. Barstow, A. Kabuth, and M. T. Pontes, "Assessing the global wave energy potential," in *International Conference on Offshore Mechanics and Arctic Engineering*, vol. 49118, 2010, pp. 447–454.

[2] *IRENA: Innovation Outlook: Ocean Energy Technologies*. Abu Dhabi, UAE: International Renewable Energy Agency, 2020.

[3] "Electricity production by source, world," https://ourworldindata.org/grapher/electricity-prod-source-stacked, 2022, accessed on: 23/7/2023.

[4] J. V. Ringwood, S. Zhan, and N. Faedo, "Empowering wave energy with control technology: Possibilities and pitfalls," *Annual Reviews in Control*, 2023.

[5] F. Mosquera, N. Faedo, C. A. Evangelista, P. F. Puleston, and J. V. Ringwood, "Energy-maximising tracking control for a nonlinear heaving point absorber system commanded by second order sliding modes," in *IFAC CAMS, Lyngby, Denmark*, vol. 55, no. 31, 2022, pp. 357–362.

[6] N. Faedo, F. D. Mosquera, C. A. Evangelista, J. V. Ringwood, and P. F. Puleston, "Preliminary experimental assessment of second-order sliding mode control for wave energy conversion systems," in *2022 Australian & New Zealand Control Conference (ANZCC)*. IEEE, 2022, pp. 63–68.

[7] R. H. Hansen and M. M. Kramer, "Modelling and control of the wavestar prototype," in *Proceedings of the 9th European Wave and Tidal Energy Conference, EWTEC 2011*. University of Southampton, 2011.

[8] N. Faedo, Y. Peña-Sanchez, E. Pasta, G. Papini, F. D. Mosquera, and F. Ferri, "Swell: An open-access experimental dataset for arrays of wave energy conversion systems," *Renewable Energy*, vol. 212, pp. 699–716, 2023.

[9] N. Faedo, Y. Peña-Sanchez, E. Pasta, G. Papini, F. Mosquera, and F. Ferri, "Swell: An open-access experimental dataset for arrays of wave energy conversion systems," Mendeley Data, 2023.

[10] A. Levant, "Sliding order and sliding accuracy in sliding mode control," *Int. J. Control*, vol. 58, no. 6, pp. 1247–1263, 1993.

[11] M. A. Golkani, S. Koch, R. Seeber, M. Reichhartinger, and M. Horn, "An anti-windup scheme for the super-twisting algorithm," in *2019 IEEE 58th Conference on Decision and Control (CDC)*. IEEE, 2019, pp. 6947–6952.

[12] Y. Shtessel, C. Edwards, L. Fridman, and A. Levant, *Sliding Mode Control and Observation*. Springer New York, 2013.

[13] A. Ferrara and M. Rubagotti, "A sub-optimal second-order sliding mode controller for systems with saturating actuators," *IEEE Transactions on Automatic Control*, vol. 54, no. 5, pp. 1082–1087, May 2009.

[14] I. Castillo, M. Steinberger, L. Fridman, J. A. Moreno, and M. Horn, "Saturated super-twisting algorithm: Lyapunov based approach," in *14th International Workshop on Variable Structure Systems (VSS)*, June 2016, pp. 269–273.

[15] I. Castillo, M. Steinberger, L. Fridman, J. Moreno, and M. Horn, "Saturated super-twisting algorithm based on perturbation estimator," in *IEEE 55th Conference on Decision and Control (CDC)*, Dec 2016, pp. 7325–7328.

[16] R. Seeber and M. Reichhartinger, "Conditioned super-twisting algorithm for systems with saturated control action," *Automatica*, vol. 116, pp. 108 921: 1–9, 2020.

[17] D. García-Violini, Y. Peña-Sanchez, N. Faedo, C. Windt, F. Ferri, and J. V. Ringwood, "Experimental implementation and validation of a broadband LTI energy-maximizing control strategy for the Wavestar device," *IEEE Tran. on Control Sys. Tech.*, vol. 29, no. 6, pp. 2609–2621, 2021.

[18] L. Papillon, R. Costello, and J. V. Ringwood, "Boundary element and integral methods in potential flow theory: a review with a focus on wave energy applications," *Journal of Ocean Engineering and Marine Energy*, pp. 1–35, 2020.

[19] D. García-Violini, Y. Peña-Sanchez, N. Faedo, F. Ferri, and J. V. Ringwood, "A broadband time-varying energy maximising control for wave energy systems (lite-con+): Framework and experimental assessment," *IEEE Transactions on Sustainable Energy*, 2023.

[20] L. Ljung, *System Identification: Theory for the User*, ser. Prentice Hall information and system sciences series. Prentice Hall PTR, 1999.

[21] T. McKelvey, H. Akçay, and L. Ljung, "Subspace-based multivariable system identification from frequency response data," *IEEE Transactions on Automatic control*, vol. 41, no. 7, pp. 960–979, 1996.

[22] S. Boyd and L. Vandenberghe, *Convex optimization*. Cambridge university press, 2004.

[23] N. Faedo, "Optimal control and model reduction for wave energy systems: A moment-based approach," Ph.D. dissertation, Department of Electronic Engineering, Maynooth University, 2020.

[24] N. Faedo, Y. Peña-Sanchez, and J. V. Ringwood, "Receding-horizon energy-maximising optimal control of wave energy systems based on moments," *IEEE Transactions on Sustainable Energy*, vol. 12, no. 1, pp. 378–386, 2020.

[25] R. Hanus, M. Kinnaert, and J.-L. Henrotte, "Conditioning technique, a general anti-windup and bumpless transfer method," *Automatica*, vol. 23, no. 6, pp. 729–739, 1987.